PREDICTED SURFACE VOLATILE AND SUBSURFACE WATER ICE THERMAL STABILITY ZONES AT THE LUNAR POLES FROM DIVINER DATA. M.E. Landis[1*], P.O. Hayne[1], J.-P. Williams[2], B.T. Greenhagen[3], D.A. Paige[2]. [1]Laboratory for Atmospheric and Space Physics, University of Colorado, Boulder, CO, USA (*margaret.landis@lasp.colorado.edu), [2]Department of Earth, Planetary and Space Sciences, University of California, Los Angeles, CA, USA, [3]Johns Hopkins University Applied Physics Laboratory, Laurel, MD, USA.

Introduction: The source of lunar polar volatiles has been a long-standing problem in planetary science. Direct measurements and inferences from remote sensing have indicated that water ice and other volatiles exist in the near-subsurface of the lunar south polar region (e.g., [1-6]). Neutron data suggest hydrogen enhancement at both poles (e.g., [7]), consistent with the presence of buried water ice or hydrated minerals in the upper ~1 m of the surface. Buried water ice has been suggested to explain trends in lunar crater depth-to-diameter ratios with latitude [8] and could record previous lunar polar orientations [9]. While the presence and role of water and possibly other ices in the lunar polar regions has been explored through numerous datasets, key questions remain unanswered, including the sources and supply rates of volatiles over time. Knowledge of the distribution of cold-traps where diverse volatiles may be sequestered is critical for modeling and understanding the cold-trapping process, and will also help guide future missions investigating potential sources of volatiles at the lunar poles.

We use Diviner lunar radiometer [10] data to determine bolometric temperatures at a 0.01° scale from 60 to 90° latitude in both hemispheres to better understand the locations where volatiles would be thermally stable, if present, at the surface and in the subsurface. We use maximum annual temperature to quantify surface volatile thermal stability, and annual average bolometric temperatures to infer where water ice would be thermally stable within ~1 m of the surface. We present the results of the surface volatile thermal stability, initial results from subsurface stability modeling, and implications for future exploration.

Data and methods: In order to determine annual maximum temperatures for surface thermal stability, we used 10 Draconic years of Diviner radiance data (2009-2019) and process it according to [1] as summarized in [11]. We use the volatile <1 mm/Gyr sublimation temperatures given in [12] as temperature cutoffs for the stability of the condensed volatile. We generate volatile maps for all the volatiles listed in [12] in [11], and present a subsection here in Fig. 1.

For subsurface volatile stability, we determined the annual average bolometric temperature for each pixel in the temperature map. We find the average radiance over 10 Draconic years in each map pixel, then convert radiances to bolometric temperature using the standard method described in [1]. The assumption that the annual average temperature is equal to the subsurface temperature (< 1 m) is accurate, provided that the diurnal and annual skin depths are smaller than ~1 m, and that polar temperatures are generally low enough that thermal effects on conductivity (e.g., [13]) are negligible.

Surface volatile stability: We track three volatiles (sulfur S_1, water, and hydrogen cyanide) whose relative abundances would provide insight into the long-term supply sources for the volatiles at the lunar poles. Results at three locations, one at the north pole and two at the south, in Figure 1. These areas where volatiles from volcanic outgassing (S_1, water), solar wind generation (water), and cometary delivery (water and trace organics) would all be thermally stable at the surface and therefore provide areas of high exploration interest. If present, these volatiles

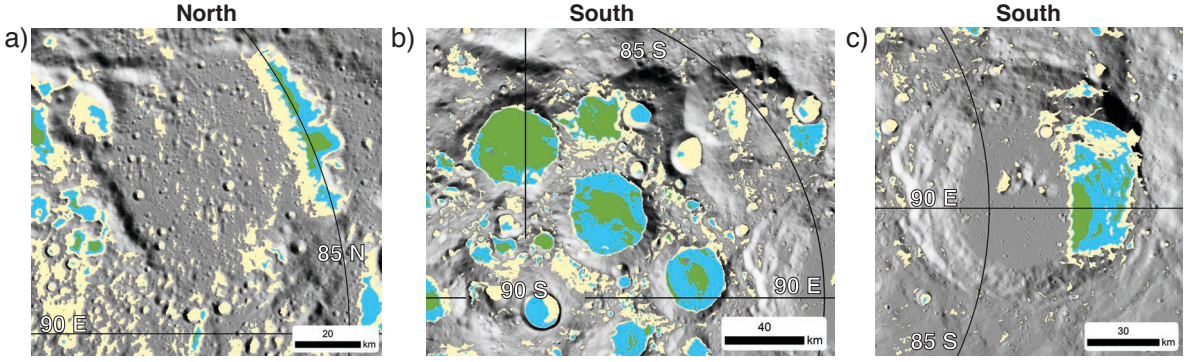

Figure 1 The locations of predicted surface thermal stability of sulfur (yellow), water (blue), hydrogen cyanide (green), and CO_2 (purple) a) Rozhdestvenskiy W crater at the north pole, b) Haworth, Shoemaker, and Faustini craters at the south pole, and c) Amundsen crater at the south pole.

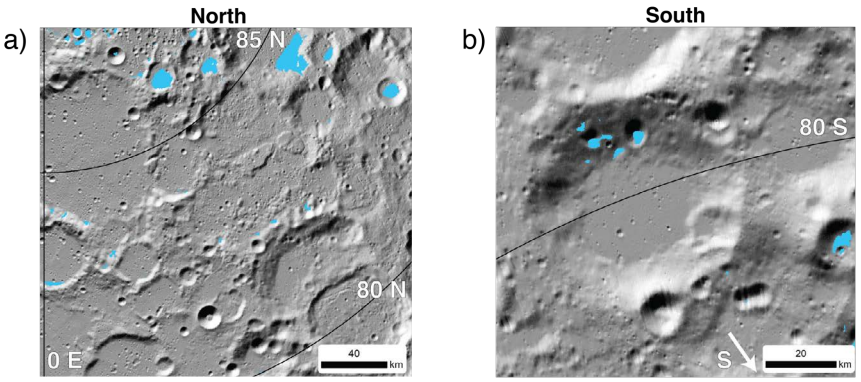

Figure 2 a) Region of the north polar near-side that includes of Nansen A (~82° N, 64° E) and De Sitter M (~81°N, 67° E) craters where surface water ice deposits would be thermally stable. b) Small impact craters on the rim of Newton A provide locations <107 K where water ice would be thermally stable.

could indicate the relative contribution of different mechanisms of volatile delivery to the Moon. If they are not present, thermal loss is unlikely to be a dominant cause compared to erosion mechanisms like photolysis and micrometeorite bombardment.

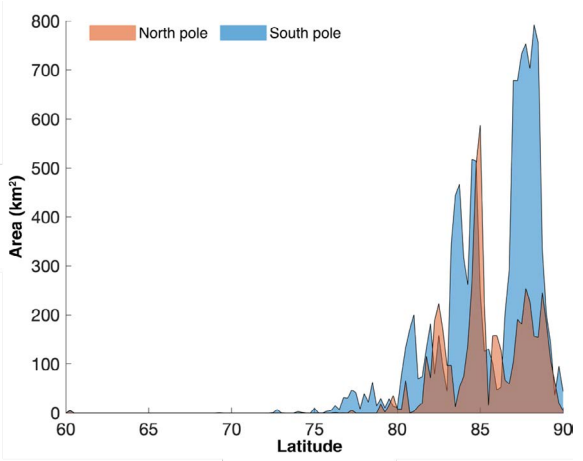

Figure 3 Area in square kilometers versus latitude for surface thermal water ice stability for the north (red) and south (blue) poles.

We map where water ice surface thermal stability areas are predicted to be at their most equatorward latitudes (Fig. 2), some < 80° latitude. These locations are mostly in smaller craters. These craters are generally more frequently produced than larger, km-scale craters, indicating that there may be a broader range of ages of these water ice thermal stability regions than in larger permanently shadowed regions.

Finally, we plot the area in 2.5° latitude bins where water ice would be thermally stable on the surface based on Diviner data (Fig. 3). The north has significantly less total area for surface water ice thermal stability than in the south, though more of the stable area is concentrated at lower latitudes in the north. This hemispheric asymmetry is observed to be a consequence of the difference in km-plus scale topography from impact craters at the two poles, and additional unmapped small cold-trap areas are likely due to smaller-scale roughness (e.g., [14]).

Subsurface water ice stability: Assuming annual average temperatures are representative of temperatures in the ~1 m of the surface, we use 145 K as a preliminary cutoff for water ice stability on airless bodies (e.g., [15]) (Fig. 4). We will expand data to 60° to 90° latitude at both poles, refine the subsurface water ice stability model, and present the results at the conference.

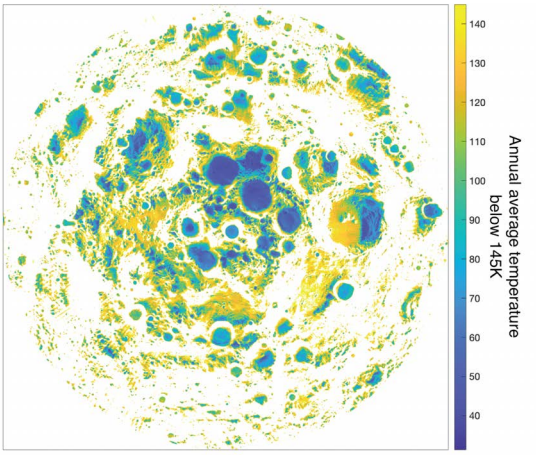

Figure 4 Regions at the lunar south pole from 80-90° S where annual average temperature is <145 K.

Acknowledgments: This work has been supported by NASA's Lunar Reconnaissance Orbiter (LRO) Diviner and the Lunar Flashlight programs. We acknowledge the helpful advice of M. Sullivan in processing these data sets.

References: [1] Paige, D.A., et al. (2010). *Science*, 330(6003) [2] Colaprete, A., et al. (2005). *Nature*, 435 [3] Hayne, P.O., et al. (2010). *Science*, 330(6003) [4] Pieters, C.M., et al. (2009). *Science*, 326(5952) [5] Schultz, P.H., et al. (2010). *Science*, 330(6003) [6] Sefton-Nash, E., et al. (2019). *Icarus*, 332 [7] Feldman, W.C., et al. (1998). *Science*, 281(5382) [8] Rubanenko, L., et al. (2019). *Nat. Geo.*, 12(8) [9] Siegler, M.A., et al. (2016). *Nature*, 531(7595) [10] Paige, D.A., et al. (2010). *SSR*, 150(1-4) [11] Landis et al. (accepted), *PSJ* [12] Zhang, J.A., et al. (2009). *GRL*, **36**(16) [13] Schorghofer, N., et al. (2007). *JGR: Planets*, 112(E2) [14] Hayne, P.O., et al. (2021). *Nat. Astro*, 5(2) [15] Hayne, P.O., et al. (2015). *JGR: Planets*, **120**(9)